International Journal of Technology (2015) 4: 594-603
ISSN 2086-9614

NUMERICAL SIMULATION OF A TWO-BED SOLAR-DRIVEN ADSORPTION CHILLER IN A TROPICAL CLIMATE

Nasruddin[1*], Lemington[1], Muhammad Idrus Alhamid[1]

[1] *Department of Mechanical Engineering, Faculty of Engineering, Universitas Indonesia, Kampus Baru UI Depok, Depok 16424, Indonesia*

(Received: June 2015 / Revised: September 2015 / Accepted: October 2015)

ABSTRACT

Cooling systems in tropical countries consume a large part of energy usage in a building, especially in a tropical climate, which places a high demand on cooling systems throughout the year. This paper presents a simulation of a two-bed silica gel-water adsorption chiller, utilizing solar energy based in the tropical climate of Indonesia. The adsorption chiller is being mathematically modelled and calculated numerically using MATLAB®. The simulation is used to show the performance of the chiller during the working hours, based on maximum and minimum inputs of solar irradiation in Indonesia Furthermore, mass recovery and heat recovery is also applied in the adsorption cycle in order to increase the cooling capacity. The adsorption chiller is based on the most recent chiller developed by Shanghai Jiao Tong University (SJTU). The simulation results generally demonstrated the running characteristics of the chiller under a range of different values of solar radiation. Furthermore, the simulation results in detail showed that during the maximum value of irradiation, the average value of COP can reach 0.26, while during the minimum value of irradiation the COP is 0.15. At the same time, the cooling capacity is also varied which can reach up to the maximum value of 37.8 kW, whereas in the minimum range of irradiation values, the cooling capacity dropped to 5.3 kW.

Keywords: Adsorption chiller; Indonesia climate; Silica gel

1. INTRODUCTION

Air-conditioning technology has been dominated by vapor compression systems. A vapor compression system uses a huge amount of electricity to drive the compressor. Besides electrical consumption, a vapor compression system also contributes to global warming because of CFC and HCFC gas refrigerants. On the other hand, according to Wang et al. (2013) 41% of global energy consumption is attributed to building useage, of which 33% use air-conditioning systems.

As a method to substitute CFC and HCFC gas, adsorption technology has attracted many researchers (Fernandes et al., 2013). Besides being able to utilize natural refrigerants, the system also can use waste heat from industrial activities or from solar heat gain. Looking at the high level of solar irradiation in Indonesia, which can reach 1,000 W/m^2 on average at the ground surface during mid-day (Jacobs, 2010), solar energy is highly feasible to be utilized in Indonesia. Moreover, Indonesia, as a tropical country, has a continuous irradiation throughout the year. At the same time, the air-conditioning needs are also continuous all year long. Adsorption cooling system can be defined by heat input temperatures, ranging from 50–600^{o}C

* Corresponding author's email: nasruddin@eng.ui.ac.id, Tel.+62-21-7270032, Fax. +62-21-7270033
Permalink/DOI: http://dx.doi.org/10.14716/ijtech.v6i4.1333

(Wang et al., 2006). Therefore, it is suitable to utilize solar energy even though the temperature ranges vary throughout the day. In addition, an adsorption system has several advantages, including simple control mechanisms, low operating costs and lower vibration levels (Pan et al., 2014). Those advantages will help the system to be more promising when applied in near future. However, adsorption systems are still facing low COP problems (Wang et al., 2006). Therefore, the size of the chiller system becomes oversized, heavy and unwieldly.

In the past twenty years, adsorption cooling systems have been studied, as a basic simulation model to analyze the operating conditions of a two-bed silica gel-water adsorption chiller (Saha et al., 2006). Then, some researchers at Shanghai Jiao Tong University (SJTU) also investigated and did some experimental work in developing adsorption chillers using working pairs and varieties of heat sources (Wang et al., 2014). Simulation models were developed based on the SJTU developed chiller, which provided operating characteristics and some initial conditions for a solar energy powered chiller (Zhang et al., 2011). Besides, this simulation revealed the fact that a longer duration of hot water circulation can result in better chiller performance. Recent studies include using a modular type adsorbent chiller system, which can greatly reduce the cost of manufacturing, (Pan et al., 2014). These research examples provide the basic rationale for simulation and investigation of an adsorption chiller trial case study, located in Indonesia's tropical climate conditions.

In this paper, an adsorption chiller based on a model from SJTU built by Pan et al. (2014) is being simulated utilizing weather data in Depok, Indonesia. The performance of the chiller is apparent in the results, which analyzed the input of maximum and minimum solar irradiation during the day. The final data will be shown to consider the application of adsorption chillers in tropical regions.

2. SYSTEM DESCRIPTION

The adsorption chiller is based on the most recent model developed in SJTU by Pan et al. (2014). The Schematic of an Adsorption Chiller (Figure 1) shows the schematic of the model chiller. The chiller contains 2 adsorbers, 2 condensers, and 2 evaporators.

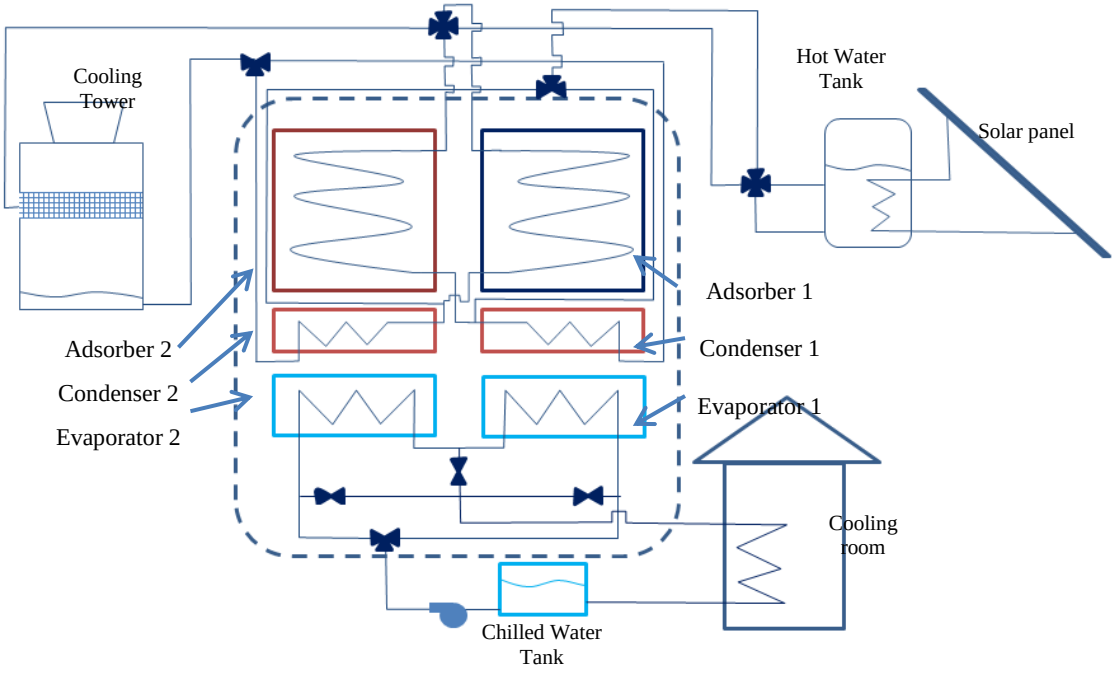

Figure 1 Schematic of Adsorption Chiller

In order to improve the reliability of the chiller, vaccum valve is not adopted in this model. The adsorber is built using a modular type of adsorber, which is composed of a fin-tube heat exchanger immersed in the silica gel.

The condenser and evaporator are both tube heat exchangers. The control system uses an automatic control with a time-based valve control. The solar panel and cooling tower is the additional component as the heat source and cooling water circulation necessary used. In addition, the operating mode is applied to mass recovery with a heat recovery mode using valve controls. The detail operating mode is described in Pan et al. (2014).

3. MATHEMATICAL MODEL

The mathematical model is developed based on heat transfer calculations at heat balance points located at every inlet and outlet position. The simulation constants are based on properties, which are shown in Table 1. The simulation also assumes simplification to limit unnecessary conditions, (Wang et al., 2005), such as:

1. There are neither pressure nor temperature drops along the pipe.
2. The shell that covers the chiller is absolutely isolated.
3. The high performance cooling tower output is always in the same temperature.
4. The adsorbent is adsorbed homogenously in every part of the adsorber, since the pressure difference is negligible.
5. The adsorption/desorption process is considered as fully isobaric.

3.1. Adsorption Rate Equation

A non-equilibrium adsorption equation is developed using a kinetic rate equation based on the diffusion rate of the water vapor (Zhang et al., 2011; Wang et al., 2006; Miyazaki et al., 2009), as follows:

$$\frac{dx}{dt} = \frac{15\ D_{so}\ \exp\left(\frac{-Ea}{R.T_b}\right)}{R_p^2}(x^* - x) \tag{1}$$

where x^* refers to the equilibrium capacity in the adsorber, that can be calculated using a adsorption equilibrium equation, which is known as the modified Freundlich equation (Zhang et al., 2011; Miyazaki et al., 2009), as follows:

$$x^* = A(T_s)\left[\frac{P_s(T_w)}{P_s\ (T_b)}\right]^{B(T_b)} \tag{2}$$

where A and B are calculated using experimental numerical values that are shown as follows (Miyazaki et al., 2009):

$$A(T) = A_0 + A_1T + A_2T^2 + A_3T^3 \tag{3}$$

$$B(T_b) = B_0 + B_1T + B_2T^2 + B_3T^3 \tag{4}$$

Then, the saturation pressure is defined using the equation (Wang et al., 2006):

$$\begin{aligned} P_s(T) = {} & 0.0000888(T - 273.15)^3 - 0.0013802(T - 273.15)^2 \\ & + 0.0857427(T - 273.15) + 0.4709375 \end{aligned} \tag{5}$$

3.2. Energy Balance for Adsorber

The energy balance for the adsorber is based on the heat exchange equation (Zhang et al., 2011), which is:

$$\begin{aligned} &\frac{dT_b}{dt}\left[M_{ad}\left(C_{ad}+C_{p,w}X\right)+C_{Cu}\,M_{tube,ad}+C_{Al}\,M_{fin,ad}\right] \\ &=\ M_{ad}\,\Delta H\,\frac{dx}{dt}+\ \dot{m_{hw}}\,C_{p,w}\left(T_{ad,in}-\ T_{ad,out}\right) \\ &-\delta\,M_a C_{w,v}\ \left(T_b-\ T_e\right)\frac{dx}{dt} \end{aligned} \tag{6}$$

where δ is act as a logic value which is:

δ = 1 is for an adsorption process, and δ = 0 is for a desorption process (7)

The first term in the left part of Equation 6 refers to the heat energy exchanged in the fin-tube heat exchanger as the adsorber. On the other hand, the second term shown in the equation's right part indicates the energy in the refrigerants that exchanges the heat in the adsorber.

At the same time, the temperature difference occuring in the adsorber is calculated using LMTD method which can be expressed as:

$$\frac{T_{ad,out}-T_b}{T_{ad,in}-T_b}=\exp\frac{-U\,A_{ad}}{\dot{m_{hw}}\,C_{p,w}} \tag{8}$$

3.3. Energy Balance for the Condenser

The same equation is developed for the condenser based on the heat exhange equation, which is:

$$\begin{aligned} M_c\,C_{Cu}\,\frac{dT_c}{dt}=(1-\delta)\Big[-L\,M_a\,\frac{dx}{dt}+\ C_{w,v}\ M_a\frac{dx}{dt}\,(T_c-\ T_b) \\ +\dot{m_{cool}}\ C_{p,w}\left(T_{cool,in}-\ T_{cool,out}\right)\Big] \end{aligned} \tag{9}$$

As the condenser is placed below the adsorber and above the evaporator, therefore there is no liquid refrigerant remaining in the condenser. The refrigerant directly drops into the evaporator after being condensed. Consequently, Equation 9 only used for the condenser during the desorption cycle.

Similar to the adsorber energy balance, the temperature of refrigerant in the condenser can also be defined by the LMTD method:

$$\frac{T_{cool,out}\ -\ T_c}{T_{cool,in}\ -\ T_c}=\exp\frac{-U\,A_c}{\dot{m_{cool}}\ C_{p,w}} \tag{10}$$

3.4. Energy Balance for Evaporator

Similar to the energy balance in the condenser, the structure of the evaporator is also similar to the condenser. As a result, the energy balance is expressed as:

$$\frac{d\,T_e}{dt}\left[M_{e,w}\,C_{p,w}+C_{Cu}\,M_e\right] = \delta\left[-L\,M_a\,\frac{dx}{dt}+\dot{m_{chill}}\,C_{p,w}\left(T_{chill,in}-T_{chill,out}\right)\right] + (1-\delta)\left[\theta\,C_{p,w}(T_e-T_c)\,M_a\frac{dx}{dt}-(1-\theta)L\,M_a\,\frac{dx}{dt}\right] \quad (11)$$

where θ is a flag equation, which has a value of:

$$\theta = 1 \text{ if } T_c \le T_e \text{ , while } \theta = 0 \text{ if } T_c > T_e \quad (12)$$

$$\frac{T_{chill,out}-T_e}{T_{chill,in}-T_e} = \exp\frac{-U\,A_e}{\dot{m_{chill}}\,C_{p,w}} \quad (13)$$

When the evaporator is not working, the refrigerant is left in the bottom of the chiller. Therefore, heat exchange also occurs during the desorption cycle. Changes in mass and temperature also occur in the liquid refrigerant inside the evaporator. These changes can be defined as a proportional value to the refrigerant capacity in the adsorber as shown in Equation 14.

$$\frac{dM_{e,w}}{d\tau} = -M_a\frac{dx}{d\tau} \quad (14)$$

3.5. Solar Energy Utilization

Solar energy is being used to produce the heated water in order to desorb water from the adsorber. Calculation of solar energy is simplified using an energy balance equation (Zhang et al., 2011), as shown in Equation 15.

$$q = \eta\,A_{solar\ panel}\,J \quad (15)$$

The heat from the solar panel is transferred to the hot water held in a tank. The energy balance is calculated as shown in Equation 16.

$$C_{p,w}\;M_{hwt,w}\,\frac{dT_{h,in}}{dt} = q + \dot{m_{hw}}\,C_{p,w}\left(T_{h,in}-T_{h,out}\right) \quad (16)$$

3.6. Mass Recovery and Heat Recovery

Mass recovery happens in the chiller when chilled water flows to the inactive evaporator before it enters the adsorption part of evaporator. In this case, the temperature of the inactive evaporator will drop significantly. As a result, the heat balance in the evaporator adds another term to evaporator energy balance equation shown in Equation 17.

$$\frac{d\,T_e}{dt}\left[M_{e,w}\,C_{p,w}+C_{Cu}\,M_e\right] = \delta\left[-L\,M_a\,\frac{dx}{dt}+\dot{m_{chill}}\,C_{p,w}\left(T_{chill,in}-T_{chill,out}\right)\right] + (1-\delta)\left[\theta\,C_{p,w}(T_e-T_c)\,M_a\,\frac{dx}{dt}-(1-\theta)L\,M_a\,\frac{dx}{dt}\right] - (1-\zeta)\left[C_{p,w}\left(T_{chill,in}{}'-T_{chill,in}\right)\right] \quad (17)$$

where $T_{chill,in}{}'$ is the chilled water outlet temperature, after the chilled water flows through the inactive evaporator, and ζ represents the flag values of 1 and 0, when the evaporator is active and inactive, respectively.

Besides this condition, the heat recovery is described during the transition cycle when it changes in one bed from the adsorption cycle to the desorption cycle, as well as to the other bed in reverse. The heat recovery cycle occurs when the adsorption bed cooled water flows into the heat water tank, and the desorption bed hot water flows to the cooling tower. In this equation there is no change in the energy balance, however there are substitute variables as shown in Equations 18 and 19:

$$T_{ad,out,ads} = T_{ad,in,des} \tag{18}$$

$$T_{cool,out} = T_{ad,out,des} \tag{19}$$

3.7. Performance Equation

The performance is judged using the most common parameter which is COP. The COP is calculated using a basic formula that is the ratio between the cooling capacity (Q_r) and heating power (Q_h) as shown in Equations 20, 21 and 22.

$$Q_r = \frac{\int_0^{t_{cycle}} C_{p,w}\, \dot{m}_{chill} \left(T_{chill,in} - T_{chill,out}\right) dt}{t_{cycle}} \tag{20}$$

$$Q_h = \frac{\int_0^{t_{cycle}} C_{p,w}\, \dot{m}_{hw} \left(T_{h,in} - T_{h,out}\right) dt}{t_{cycle}} \tag{21}$$

$$COP = \frac{Q_r}{Q_h} \tag{22}$$

4. SIMULATION PROCEDURE

Simulation is being done using MATLAB® by the Euler numerical method. The equation is being calculated every second to generate the running characteristics that are shown in Figures 3 to 5, respectively. The input parameters are based on the values shown in Table 1. Moreover, the heat input by solar energy is based on the weather data presented in Figure 2, which contain the daily climate data in Depok, Indonesia, as representative of urban tropical climatic data. The weather data are based on an average daily value for 1 year. The working hours are assumed to be 8:00 h to 17:00 h. Therefore, the data are defined as 230 W/m^2 as the minimum value and 700 W/m^2 as the maximum value, respectively.

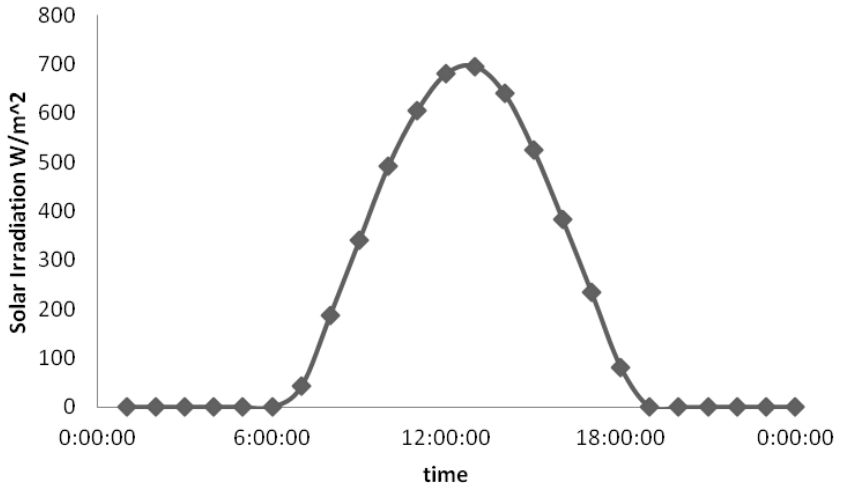

Figure 2 Daily solar irradiation in Depok, Indonesia

Table 1 Parameter of simulation

Parameters	Value	unit
Ac	400	m^2
H	0.35	%
C_a	924	J/kg ^oC
C_{al}	905	J/kg ^oC
C_{cu}	386	J/kg ^oC
$C_{p,w}$	4180	J/kg ^oC
$C_{w,v}$	1850	J/kg ^oC
D_{so}	2.54×10^{-4}	m^2/s
Ea	4.2×10^4	J/mol
ΔH	2.8×10^6	J/kg
UA_{ad}	51315	W/ ^oC
UA_c	79326.5	W/ ^oC
UA_e	35352.6	W/ ^oC
L	2.5×10^6	J/kg
Ma	342	Kg
M_{tube}	94.85	Kg
M_{fin}	48.8	Kg
M_c	172.62	Kg
M_e	471.68	Kg
R	8.314	J/mol ^oC
Rp	5×10^{-4}	M
$\dot{m_{hw}}$	6.8055	Kg/s
$\dot{m_{chill}}$	2.63888	Kg/s
$\dot{m_{cool}}$	9.583	Kg/s
$M_{hwt,w}$	2180	Kg

Simulation conditions are prepared under experimental conditions (Pan et al., 2014). Even though the experiment beforehand used a stable heat source, this simulation is considered under the same parameters. The simulation is conducted with the following varibales: 600s cooling time, 40s mass recovery and 24s heat recovery. In addition, the ambient temperature is considered to be 30^{o}C. At the beginning, the hot water temperature is defined as 60^{o}C, which is considered to be the minimum temperature for hot water to start the chiller. The simulation is running for 10 cycles in order to achieve a steady condition.

5. RESULTS AND DISCUSSION

5.1. Running Characteristics at Minimum Value of Irradiation

The running characteristics for irradiation value are about 230 W/m^2 as shown in Figures 3(a) and 3(b). Figure 3(a) illustrates the temperature at every outlet. In Figure 3(a), the temperature of the hot water input is quite stable, which means the heat input from solar energy is a balanced value to overcome the heat necessary to desorb. On the other hand, the temperature of hot water outlet, cooling water outlet, and chilled water outlet are on average 59.73^{o}C, 31.62^o C, and 11.51^{o}C, respectively. Figures 3(a) and 3(b) also show the fluctuation of temperature reached during the transition time.

Figure 3(b) demonstrates the cooling capacity during the cycle. Generally the cooling capacity increases sharply when the adsorption begins, then it decreases slowly to a value of 5.3 kW. In the transition time, it drops back and then increases when the mass recovery mode starts. However, in mass recovery mode, the cooling capacity is still in a negative position. As a result, the COP is quite low at this low heat input mode. The COP of this cycle is also very low, at

about 0.15. From the beginning, there is no improvement in stable hot water input, so the COP will not increase.

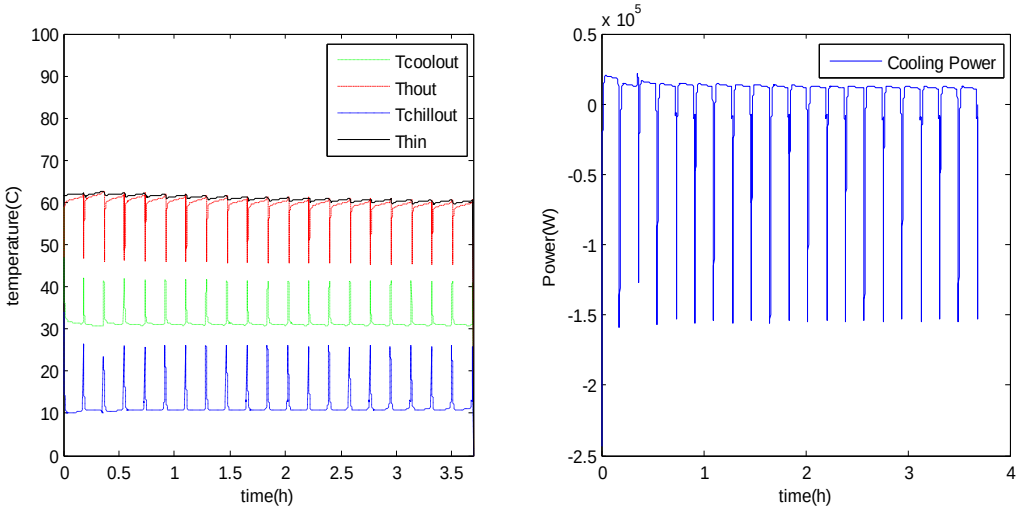

(a) (b)

Figure 3 Running characteristics for solar heat input of 230 W/m^2: (a) Temperature; (b) Cooling Capacity

5.2. Running Characteristics at a Maximum Value of Irradiation

At the maximum irradiation of 700 W/m^2, the running characteristics are different as shown in Figure 4(a), in which the hot water input is increased to 90^{o}C, then it is stopped by the system to avoid the water boiling inside the hot water tank. According to the running characteristics, the hot water is being heated for about 2.5 hours until it reaches a stable hot water temperature. This increment is followed by the hot water outlet temperature, which in the beginning is about 60^{o}C then it increases to reach 87^{o}C. Followed by the high heat input, the chilled water temperature is then lowered to increase the cooling capacity, which reaches 8.6^{o}C at the chilled water outlet.

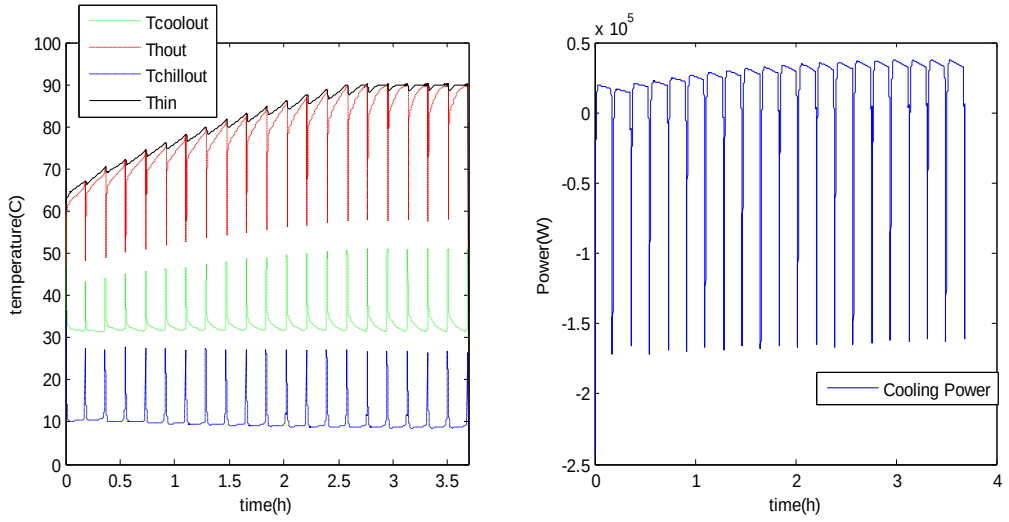

(a) (b)

Figure 4 Running characteristic for solar heat input of 700 W/m^2: (a) Temperature; (b) Cooling Capacity

In case of the cooling capacity as shown in Figure 4(b), the cooling capacity is low at the beginning along with a low temperature at the hot water inlet. Then the cooling capacity increases significantly until it reaches 37.4 kW at the highest temperature from the heat source.

At the mass recovery mode, the cooling capacity drops to a lower level, but in contrast to the characteristics occurring at the minimum radiation, the cooling capacity is still positive. At the mass recovery mode, the chiller still can cool the room. The COP of these 10 cycles is about 0.26. In the following cycles, it is predicted that a higher COP can be achieved. This prediction is caused by the high heat source that is different from those conditions at the beginning of the cycle. In other words, the chiller has to be maintained at the high temperature of hot water inlet to maximize the efficiency.

6. CONCLUSION

The simulation of silica gel-water adsorption chiller driven by solar energy is based on being in a tropical climate with Indonesia is being developed and investigated in this research. Its aim is to increase the use of adsorption chillers in Indonesia. Different solar irradiation is being simulated to determine the running characteristics of adsorption chillers in a tropical climate. The conclusions are as follows: Tropical regions typically have high solar irradiation, coupled with high demand for cooling from buildings throughout the year, which prompts the simulation of an adsorption chiller in Indonesia. The running characteristics of the adsorption chiller show that the minimum value of solar irradiation during working days can reach the cooling capacity of 5.3 kW, however the COP is very low at a value of 0.15. On the other hand, the chiller works well at the maximum value when it reaches the cooling capacity of 37.4 kW and a COP rating of 0.26, which is predictably higher with increasing cycles.

7. ACKNOWLEDGEMENT

The author would like to thank Mr. Pan Quanwen and Prof. Wang Ruzhu for his assistance, guidance and experience in the experiment at SJTU. This work is supported by Indonesian National Research Fund for Higher Education (HIBAH PUPT DIKTI) in 2015 under the Contract number: 0577/UN2.R12/HKP.05.00/2015.

8. NOMENCLATURE

Ac	area of the solar collector (m^2)
A	area (m^2)
ΔH	isosteric heat of adsorption (J kg^{-1})
COP	Coefficient of performance
C	Specific heat (J kg^{-1} $^oC^{-1}$)
Ea	activation energy (J kg^{-1})
Rp	radius of adsorbent particle (m)
L	latent heat of vaporization (J kg^{-1})
$\dot{m}$	mass flow (kg s^{-1})
M	mass (kg)
Dso	pre-exponential term (m^2s^{-1})
P	Pressure (Pa)
R	gas constant (J kg^{-1} $^oC^{-1}$)
x	adsorption capacity (kg kg^{-1})
U	heat exchanger coefficient (W m^{-2} $^oC^{-1}$)
J	solar irradiation (J m^{-2})
q	solar heating power (W)
Q	Power (W)
T	temperature (^oC)
t	time (s)
η	efficiency of solar collector

subscript

al	aluminium
ad	adsorber
b	adsorber bed
c	condenser
e	evaporator
cu	copper
chill	chilled water
cool	cooled water
h	hot water
in	inlet
out	outlet
w	refrigerant (water)
ht	hot water tank
v	water vapor

9. REFERENCES

Chua, H.T., Ng, K.C., Malek, A., Kashiwagi, T., Akisawa, A., Saha, B.B., 1999. Modelling the Performance of Two-bed, Silica Gel-water Adsorption Chillers. *International Journal of Refrigeration*, Volume 22, pp. 194–204

Di, J., Wu, J.Y., Xia, Z.Z., Wang, R.Z., 2007. Theoretical and Experimental Study on Characteristics of Novel Silica Gel-water Chiller under the Conditions of Variable Heat Source Temperature. *International Journal of Refrigeration*, Volume 30, pp. 515–526

Fernandes, M.S., Brites, G.J.V.N., Costa, J.J., Gaspar, A.R., Costa, V.A.F., 2014. Review and Future Trends of Solar Adsorption Refrigeration System. *Renewable and Sustainable Energy Reviews*, Volume 39, pp. 102–123

Jacobs, G., 2010. *Training Course on Renewable Energy Part II*, MEMR-CASINDO, Jakarta 14–18 June 2010

Miyazaki, T., Akisawa, A., Saha, B.B., El-Sharkawy, I.I., Chakraborty, A., 2009. A New Cycle Time Allocation for Enhancing the Performance of Two-bed Adsorption Chillers. *International Journal of Refrigeration*, Volume 32, pp. 864–853

Pan, Q.W., Wang, R.Z., Wang, L.W., Liu, D., 2014. Design and Experimental Study of Adsorption Chiller with Module Type Adsorber. In: *Proceedings of the International Conference of Solar Heating and Cooling for Building and Industry*, SHC 2014, Beijing, 13–15 October 2014

Saha, B.B., Boelman, E.C., Kashiwagi, T., 1995. Computational Analysis of an Advance Adsorption- refrigeration Cycle. *Energy*, Volume 10, pp. 983–994

Wang, D., Zhang, J., Tian, X., Liu, D., Sumathy, K., 2013. Progress in Silica Gel–water Adsorption Refrigeration Technology. *Renewable and Sustainable Energy Reviews*, Volume 30, pp. 85–104

Wang, D.C., Xia, Z.Z., Wu, J.Y., Wang, R.Z., Zhai, H., Dou, W.D., 2005. Study of a Novel Silica Gel-water Adsorption Chiller. Part I: Design and Performance Prediction. *International Journal of Refrigeration*, Volume 28, pp. 1073–1083

Wang, R., Wang, L., Wu, J., 2006. Adsorption Refrigeration – An Efficient Way to Make Good Use of Waste Heat and Solar Energy. *Progress in Energy and Combustion Science*, Volume 32, pp. 424–458

Wang, R., Wang, L., Wu, J., 2014. *Adsorption Refrigeration Technology Theory and Application*, Singapore: John Wiley and Sons Pte. Ltd

Zhang, G., Wang, D.C., Zhang, J.P., Han, Y.P., Sun, W., 2011. Simulation of Operating Characteristic of the Silica Gel-water Adsorption Chiller Powered by Solar Energy. *Solar Energy*, Volume 85, pp. 1469–1478